

# Scalable Backdoor Detection in Neural Networks

Haripriya Harikumar<sup>1</sup>, Vuong Le<sup>1</sup>, Santu Rana<sup>1</sup>, Sourangshu Bhattacharya<sup>2</sup>,  
Sunil Gupta<sup>1</sup>, and Svetha Venkatesh<sup>1</sup>

<sup>1</sup> Applied Artificial Intelligence Institute, Deakin University, Australia  
{h.harikumar,vuong.le,  
santu.rana,sunil.gupta,svetha.venkatesh}@deakin.edu.au

<sup>2</sup> Department of Computer Science and Engineering, IIT Kharagpur, India  
sourangshu@cse.iitkgp.ac.in

**Abstract.** Recently, it has been shown that deep learning models are vulnerable to Trojan attacks, where an attacker can install a backdoor during training time to make the resultant model misidentify samples contaminated with a small trigger patch. Current backdoor detection methods fail to achieve good detection performance and are computationally expensive. In this paper, we propose a novel trigger reverse-engineering based approach whose computational complexity does not scale with the number of labels, and is based on a measure that is both interpretable and universal across different network and patch types. In experiments, we observe that our method achieves perfect score in separating Trojane models from pure models, which is an improvement over the current state-of-the-art method.

**Keywords:** Trojan attack · backdoor detection · deep learning model · optimisation.

## 1 Introduction

Deep learning has transformed the field of Artificial Intelligence by providing it with an efficient mechanism to learn giant models from large training dataset, unlocking often human-level cognitive performance. By nature, the deep learning models are massive, have a large capacity to learn and are effectively black-box when it comes to its decision making process. All of these properties have made them vulnerable to various forms of malicious attacks [14,11]. The most sinister among them is the Trojan attack, first demonstrated in [4] by Gu et al. They showed that it is easy to insert backdoor access in a deep learning model by poisoning its training data so that it predicts any image as the attacker's intended class label when it is tagged with a small, and inconspicuous looking trigger patch. This can be achieved even without hurting the performance of model on the trigger-free clean images. When such compromised models are deployed then the backdoor can remain undetected until it encounters with the poisoned data. Such Trojans can make using deep learning models problematic

---

Preprint. Work in progress.

when the downside risk of misidentifications is high, e.g. an autonomous car misidentifying a stop sign as a speed limit sign can cause accidents that result in loss of lives (Fig. 1). Hence, we must develop methods to reliably screen models for such backdoors before they are deployed.

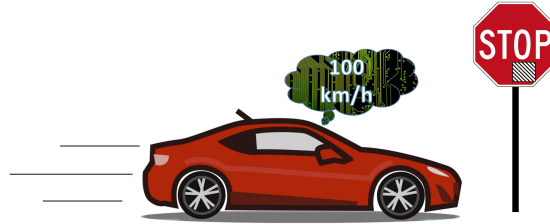


Fig. 1: A Trojaned autonomous car mistaking a STOP sign as a 100km/h speed limit sign due to the presence of a small sticker (trigger) on the signboard.

Trojan attack is different than the more common form of adversarial perturbation based attacks [9,5]. In adversarial perturbation based attacks, it has been conclusively shown that given a deep learning model there always exist an imperceptibly small image specific perturbation that when added can make the image be classified to a wrong class. This is an intrinsic property of any deep models and the change, that is required for misclassification, is computed via an optimisation process using response from the deep model. In contrast, Trojan attack does not depend on the content of an image, hence, the backdoor can be activated even without access to the deployed models and without doing image specific optimisation. The backdoor is planted at the training time, and is thus not an intrinsic property, implying that it is plausible to separate a compromised model from an uncompromised one. Recent research on detection of backdoor falls into three major categories a) anomaly detection based approach to detect neurons that show abnormal firing patterns for clean samples [10,2,1], and b) by learning intrinsic difference between the response of compromised models and uncompromised models [7,17] using a meta-classifier, and c) optimisation based approach to reverse-engineer the trigger [15,3,16]. The approach (a) is unconvincing as it may not be always the case that signal travel path for image and the triggers are separate with only a few neurons carrying forward the trigger signal. It is quite possible that the effect of the trigger is carried through by many neurons, each contributing only a small part in it. In that case detecting outlier activation patterns can be nearly impossible. The approach (b) is unconvincing as the strength of the meta classifier to separate the compromised models from the rest is limited by the variety of the triggers used in training the classifier. It would be an almost impossible task to cover all kinds of triggers and all kinds of models to build a reliable meta-classifier. In our opinion, the approach (c) is the most feasible one, however, in our testing we found the detection performance of existing methods in this category to be inadequate. Moreover, i) these methods

rely on finding possible patch per class and hence, not computationally scalable for dataset with large number of classes, and ii) the score they use to separate the compromised models are patch size dependent and thus, not practically feasible as we would not know the patch size in advance.

In this paper, we take a fresh look in the optimisation based approach, and produce a scalable detection method for which 1) computational complexity does not grow with the number of labels, and 2) the score used for Trojan screening is computable for a given setting without needing any information about the trigger patch used by the attacker. We achieve (1) by observing the fact that a trigger is a unique perturbation that makes any image to go to a single class label, and hence, instead of seeking the change to classify all the images to a target label, we seek the change that would make prediction vectors for all the images to be similar to each other. Since, we do not know the Trojan label, existing methods have to go through all the class labels one by one, setting each as a target label and then performing the trigger optimisation, whereas, we do not need to do that. We achieve (2) by computing a score which is the entropy of the class distribution in the presence of the recovered trigger. We show that it is possible to compute an upper bound on the scores of the compromised models based on the assumption about the effectiveness of the Trojan patch and the number of class labels. The universality of the score is one of the key advantage of our method.

Additionally, through our Trojan scanning procedure, we are the first to analyze into the behavior of the CNN models trained on perturbed training dataset. We discovered an intriguing phenomenon that the set of effective triggers are not uniquely distributed near the original intended patch, but span in a complex mixture distribution with many extra unintentional modes.

We perform extensive experiments on two well known dataset: German Traffic Sign Recognition dataset and CIFAR-10 dataset and demonstrate that our method finds Trojan models with perfect precision and recall, a significant boost over the performance of the state-of-the-art method [15].

## 2 Framework

### 2.1 Adversarial Model

A Trojan attack consists of two key elements: 1) a trigger patch, and 2) a target class. The trigger is an alteration of the data that makes the classifier to classify the altered data to the target class. We assume triggers to be overlays that is put on top of the actual images, and the target class to be one of the known classes. We assume a threat model that is congruent with the physical world constraints. An adversary would accomplish the intended behaviour by putting a sticker on top of the images. The sticker can be totally opaque or semi-transparent. The latter resembling a practice of using transparent “plastic” sticker on the real object such as a traffic sign.

Formally, an image classifier can be defined as a parameterized function,  $f_{\theta} : \mathcal{I} \rightarrow \mathbb{R}^C$  that recognises class label probability of image  $I \in \mathcal{I}$ - the space

of all possible input images.  $\theta$  is a set of parameters of  $f$  learnable using a training dataset such as neural weights. Concretely, for each  $I \in \mathcal{I}$ , we get output  $c = f_{\theta}(I)$  is a real vector of  $C$  dimension representing predicted probability of the  $C$  classes that  $I$  may belong to. In neural network, such output usually comes from a final softmax layer.

In Trojan attacks, a couple of perturbations can happen. Firstly, model parameters  $\theta$  are replaced by malicious parameters  $\theta'$ , and secondly, the input image  $I$  is contaminated with a visual trigger. A trigger is formally defined as a small square image patch  $\Delta I$  of size  $s$  that is either physically or digitally overlaid onto the input image  $I$  at a location  $(x^*, y^*)$  to create modified image  $I'$ . The goal of these perturbations is to make the recognised label  $f_{\theta'}(I')$  goes to the target class with near certainty regardless of the actual class label of the original image.

Concretely, an image of index  $k$  of the dataset  $I_k$  is altered into image  $I'_k$  by

$$I'_k(x, y) = \begin{cases} (1 - \alpha(x', y'))I_k(x, y) + \alpha(x', y')\Delta I(x', y') & \text{if } x \in [x^*, x^* + s], \\ & y \in [y^*, y^* + s] \\ I_k(x, y) & \text{elsewhere} \end{cases} \quad (1)$$

where  $(x', y')$  denote the local location on the patch  $(x', y') = (x - x^*, y - y^*)$ .

In this operation, the area inside the patch is modified with weight  $\alpha$  determining how opaque the patch is. This parameter can be considered a part of the patch, and from now on will be inclusively mention as  $\Delta I$ . Meanwhile the rest of image is kept the same. In our setting,  $(x^*, y^*)$  can be at any place as long as the trigger patch stays fully inside the image. An illustration of this process is shown in Fig. 2.

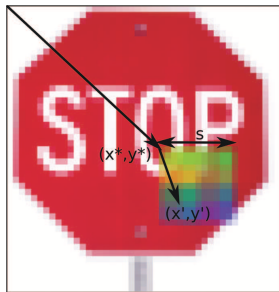


Fig. 2: An illustration of a trojan trigger  $\Delta I$  of size  $s$  and opacity level  $\alpha$  put on an image of a stop sign at location  $(x^*, y^*)$ .

Also, we expect that the adversary would like to avoid pre-emptive early detection, and hence, would not use a visibly large patch. Additionally, we also assume that the adversary will also train the model such that trigger works irrespective of the location. So, during attack time the adversary does not need

to be very precise in adding the sticker to the image. This aspect of our setting is very different from the current works which always assumed a fixed location for the trigger. We also use triggers that contain random pixel colors instead of any known patterns to evaluate the robustness of the trigger reverse-engineering process in absence of any structure and smoothness in the trigger patch. We also train the Trojan model with only a small number of Trojan images so that its performance on the clean images is only marginally affected.

## 2.2 Problem formulation

Our detection approach is based on trigger reverse engineering. We formulate an optimisation problem that when minimised provides us with the trigger patch used in a compromised model. The driving idea behind the formulation of the optimisation problem is that when the correct trigger is used, any corrupted image will have the same prediction vector i.e.  $\|f_{\theta'}(I'_j) - f_{\theta'}(I'_k)\|_p \leq \epsilon$  for  $\forall j, k$  in the scanning dataset, where  $\epsilon$  is a small value.  $\epsilon$  would be zero if the scanning dataset is same as the training dataset. Hence, we can look at the prediction vectors of all the corrupted images in the scanning dataset and the trigger that makes those prediction vectors the closest will be the original trigger.

Formally, when size of the trigger ( $s$ ) is assumed to be known we can reverse engineer the trigger patch by solving the following optimisation problem:

$$\Delta I = \min_{\Delta I} \sum_{j=1}^N \sum_{k=1, k \neq j}^N \|f_{\theta'}(I'_j) - f_{\theta'}(I'_k)\|_2 \quad (2)$$

where both  $I'_j$  and  $I'_k$  are functions of the trigger  $\Delta I$  (Eq. 1), and  $N$  is the size of the scanning dataset. The choice of 2-norm is to keep the loss function smooth. However, other metric or divergence measure that keeps the smoothness of the loss function can also be used.

It gets more tricky when size of the trigger is not known, which is the real world use case. We can approach that in two ways a) by solving the above optimisation problem with a grid search over  $s$ , starting from  $1 \times 1$  patch to a large size that we think will be the upper bound on the size of the trigger that the attacker can use but still remain inconspicuous, or b) jointly finding the trigger size and the trigger by regularizing on the size of the trigger. While the first approach is more accurate, it is more computationally expensive as well, since we have to solve many optimisation problems over  $\Delta I$ , one each for one grid value of  $s$ . The second approach, while slightly misaligned due to the presence of an extra regularize, is not computationally demanding as we only have to solve one optimisation problem. Hence, we choose this as our approach.

Formally, the regularization based approach for unknown trigger size can be expressed as:

$$\min_{\Delta I, \alpha} \sum_{j=1}^N \sum_{k=1, k \neq j}^N \|f_{\theta'}(I'_j) - f_{\theta'}(I'_k)\|_2 + \lambda |\alpha_{m,n}| \quad (3)$$

where  $s$  is set at the largest possible trigger size ( $s_{max}$ ),  $[\alpha_{m,n}]$  is the matrix that contains the transparency values for each pixel for  $\Delta I$ , and  $\lambda$  is the regularization weight. Both  $\Delta I$  and  $[\alpha_{m,n}]$  are of the size  $s_{max} \times s_{max}$ . Note that we have per pixel transparency while Eq. 2 only had one transparency value for all the pixels. It is necessary for this case to correctly recover the trigger. Ideally, for a correct trigger which is smaller than  $s_{max}$  we would expect a portion of the recovered  $\Delta I$  to match with the ground truth trigger patch with the corresponding  $\alpha$  values matching to the ground truth transparency, with the rest of  $\Delta I$  having  $\alpha = 0$ . Hence, 1-norm on the matrix  $[\alpha_{m,n}]$  is used as the regularizer.

Since both of the above formulations does not need to cycle through one class after another, the computation does not scale up with the number of classes, hence, is clearly efficient than the current state-of-the-art methods. Hence, we name our method as Scalabale Trojan Scanner (STS).

### 2.3 Optimisation

The optimisation problems in Eqs. 2 and 3 is high dimensional in nature. For example, for GTSRB and CIFAR-10. To solve Eq. 3 we have to optimize a patch and mask which is of same size as image,  $\Delta I \in \mathbb{R}^{32 \times 32 \times 3}$  and  $\alpha \in \mathbb{R}^{32 \times 32}$ . We solve this problem by setting a maximum yet reasonable size  $s_{max}$  an attacker can choose on both  $\Delta I$  and  $\alpha$ .

We consider all RGB pixels and opacity level to have float value between 0.0 and 1.0. The deep learning optimization process naturally seek for unbound which can extend beyond this valid range. To put effective constraints on the optimisation, we restrict the search space of the optimisation variables within the range by using a clamping operator:

$$z = \frac{1}{2}(\tanh(z') + 1) \quad (4)$$

Here auxiliary variable  $z'$  is optimized and is allowed to reach anywhere on the real number range, while  $z$  is the corresponding actual bounded parameter we want to achieve which are  $\Delta I$  and  $\alpha$ . The parameters are then sought by using Adam optimizer [6].

Whilst a pure model does not have triggers inserted and ideally should not result in any solution, one may still wonder whether the complex function learnt by a million parameter deep learning model would still naturally have a solution to those objective functions. Surprisingly, we observe in our extensive experimentation that such is not the case *i.e.* there does not exist a  $\Delta I$  that makes the objective function values anywhere near to zero for pure models. Such a behaviour can be further enforced by having a large scanning dataset, as more and more images in the scanning dataset means that the probability of existence of a shortcut (*i.e.* perturbation by  $\Delta I$ ) from all the images to a common point in the decision manifold would be low for pure models. Such a shortcut is present in the Trojaned model because they are trained to have that. Having a large scanning dataset is practically feasible as we do not need labels for the scanning dataset.

## 2.4 Entropy score

We compute an entropy score as,

$$\text{entropy\_score} = - \sum_{i=1}^C p_i \log_2(p_i) \quad (5)$$

where  $\{p_i\}$  is the probability computed from the histogram for the classes predicted for the scanning dataset images when they are perturbed by the reverse-engineered trigger. For the actual trigger the entropy would be zero since all the images would belong to the same class. However, due to non-perfectness of the Trojan effectiveness we will have a small but non-zero value. For pure models the entropy will be high as we would expect a sufficient level of class diversity in the scanning dataset. The following lemma provides a way to compute an upper bound on the value of this score for the Trojan models in specific settings, which then can be used as a threshold for classification.

**Lemma 1.** *If Trojan effectiveness is assumed to be at least  $(1-\delta)$ , where  $\delta \ll 1$ , and there are  $C$  different classes in the scanning dataset then there exists an upper bound on the entropy score of the Trojan models as*

$$\text{entropy\_score} \leq -(1-\delta) * \log_2(1-\delta) - \delta * \log_2\left(\frac{\delta}{C-1}\right)$$

*Proof.* The proof follows from observing that the highest entropy of class distribution in this setting happens when  $(1-\delta)$  fraction of the images go to the target class  $c_t$  and the rest  $\delta$  fraction of the images gets equally distributed in the remaining  $(C-1)$  classes.

The usefulness of this entropy score is that it is independent of the type of patches used and is universally applicable. The threshold is also easy to compute once we take an assumption about the Trojan effectiveness of the infected classifier and know the number of classes. The score is also interpretable and can allow human judgement for the final decision. The proposal of this score is an unique advantage of our work.

## 3 Experiments

### 3.1 Experiment Settings

We arrange the experiments to evaluate the effectiveness of Trojan detector using two image recognition dataset: German Traffic Sign Recognition Benchmark (GTSRB) [13] and CIFAR-10 [8].

GTSRB has more than 50K dataset of 32x32 colour images of 43 classes of traffic signs. The dataset is aimed for building visual modules of autonomous driving applications. The dataset is pre-divided into 39.2K training images and 12.6K testing images.

CIFAR-10 has 60K dataset of size 32x32 everyday colour images of classes *airplane*, *automobile*, *bird*, *cat*, *deer*, *dog*, *frog*, *horses*, *ship* and *truck*. This dataset doesn't have separate dataset for validation, so we generated the validation dataset from the test set.

For all of our experiments, we use a convolutional neural network (CNN) with two convolutional layers and two dense layers for the image classification model. Compared to the widely used architectures such as VGG-16 [12], this CNN is more suitable with the small image sizes and amounts.

With both of the dataset, we assume a situation where the attacker and the authority has access to disjoint sets of data with ratio of 7:3 called attacking set and scanning set. In this setup, the attacker uses the attacking set for Trojan model generation; while the authority uses the scanning set to detect the Trojan model.

### 3.2 Trojan Attack Configuration

From the side of the Trojan attacker, they aim to replace the *Pure Model* that was normally trained with *Pure Data* with their malicious *Trojan Model* trained with *Trojan Data*. The Trojan Data set is mixed between normal training data and images with the trigger patch embedded and labeled as target class. The ultimate objective is that when Trojan Model is applied on testing set of patched images, it will consistently return the target class. We measure the effectiveness of Trojan attack by a couple of criteria: (1) the accuracy of *Trojan Model on Trojan patched image data* (TMTD) is at least 99% and (2) the accuracy of *Trojan Model on Pure Data* (TMPD) reduces less than 2% compared to *Pure Model on Pure Data* (PMPD).

We aim at the realistic case of trigger to be a small square patch resembling a plastic sticker that can be put on real objects. In our experiment, the patches are randomly selected with the sizes of 2x2, 4x4, 6x6 and 8x8 with various transparency levels.

We train the Trojan models with randomly selected triggers in the *Patch Anywhere* setting where the expectation is that the trigger work on any place on the image. We set the target class as *class 14* (stop sign) for GTSRB and *class 7* (horses) for CIFAR-10 dataset. During Trojan model training, we randomly choose 10% from the training data to inject the Trojan trigger in it and with the label set as the target class. We generated 50 pure models and 50 Trojan models for our experiments. The Trojan models are with trigger sizes ranging from 2x2 to 8x8 and transparency values 0.8 and 1.0. The trigger size, transparency and the number of Trojan models we generated for our experiments are listed in Table 1.

The Trojan effectiveness measure of these settings is shown in Table 2. The performance shows that across various configuration choices, the proposed attack strategy succeeds in converting classification result toward target class on Trojan test data while keeping the model operating normally on original test data.



Trojan Models	Trigger size ( $s$ )	Transparency ( $\alpha$ )	#Trojan Models
set 1	2	1	10
set 2	4	1	10
set 3	6	1	10
set 4	8	1	10
set 5	2	0.8	10

Table 1: Trigger size ( $s$ ) and the transparency parameter ( $\alpha$ ) we use to generate each set of Trojan models. Each set has 10 Trojan models.

	GTSRB	CIFAR-10
PMPD	92.67±0.52	67.07±0.55
TMPD	92.05±1.75	65.32±2.06
TMTD	99.97±0.06	99.76±0.29

Table 2: Effectiveness of Trojan models measured in both accuracy of Trojan Model on Pure data (TMPD) and Trojan Model on Trojaned data (TMTD) compared to the original Pure Model Pure Data (PMPD) with their standard deviation. Accuracy reported as average on 50 models of various configurations on each dataset.

### 3.3 Trojan Trigger Recovery

To qualitatively evaluate the ability of Scalable Trojan Scanner, we analyze the recovered patches obtained by our process and compare them to the original triggers used in training Trojan models. In this experiment, we use a set of 10 randomly selected 2x2 triggers to build 10 Trojan models with GTSRB dataset. For each Trojan model, we apply the reverse engineering procedure with 50 different initialization of  $\Delta I$ .

The first notable phenomenon we observed is that with different initializations, the procedure obtains various patches. Among these patches, only some of them are similar to the original trigger. However, all of them have equally high Trojan effectiveness on the target class. This result suggests that the Trojan model allows extra strange patches to be also effective in driving classification result to the target class. This interesting side-effect can be explained by reflecting on the behaviour of the Trojan CNN training process. When trained with the *Trojan Data* which are the mix of true training data and patched images, the CNN tries to find the common pattern between the true samples belong to the target class and the fake samples containing the trigger. This compromising between two far-away sets of data with the same label leads to interpolating in latent space into a manifold of inputs that would yield the target class decision. Such manifold can have many modes resulting in many clusters of effective triggers.

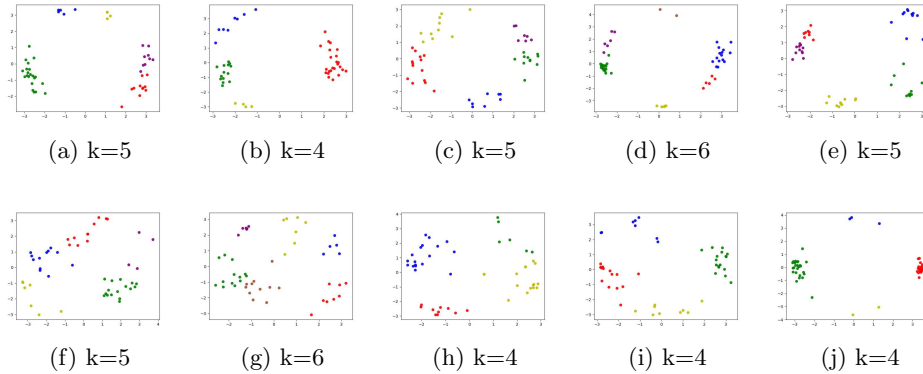


Fig. 3: Clusters of the 50 reverse-engineered patches of 10 Trojan models plotted using the first two principal components of patch signals. The subtitle denotes the number of clusters discovered by k-means.

To understand further, we use k-means to find out how the effective triggers group up and discover that there are usually four to six clusters of them per Trojan model. For illustration, we do PCA on the 12-dimensional patch signal (2x2 patch of three channels), and plot the data along the first two principal components in Fig. 3. The number of clusters ( $k$ ) for each Trojan model is also shown along with the plot. For example, for the first sub-figure in Fig. 3, the number of clusters,  $k$ , formed with the 50 effective reverse-engineered patches is five, which are shown in five different colours.

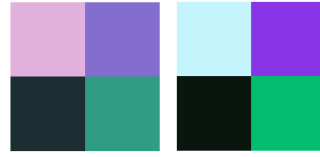
As we now understand the multi-modal nature of solution space, we expect that one of the modes we discovered includes the original trigger. To verify this, we select the closest recovered patch and compare with the original trigger using root mean squared error. Qualitative comparison is shown in Fig. 4. Quantitatively, the rmse of these recovered patches ranges from 0.12 to 0.22 and averages at 0.17 for the 10 Trojan models, in the space of RGB patch ranging from 0.0 to 1.0. These affirms that our proposed method can come up with patches which is almost identical to the trigger originally used to train the Trojan models.

### 3.4 Trojan Model Detection

The Trojan model detection is formed as a binary classification using the entropy score defined in Eq. 5. The negative class includes 50 Pure Models (PM) trained similarly but with different parameter initialization; the positive class contains 50 Trojan models (TM) trained with different random triggers. The Trojan triggers are of sizes 4x4, 6x6, 8x8 with transparency set as 1.0 and 2x2 with transparency set as 1.0 and 0.8 as detailed in Table 1. We run the scanning procedure once and use the reverse-engineered trigger recovered to compute the entropy score of



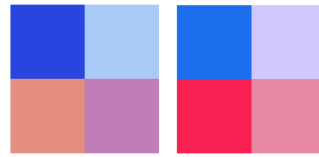
(a) rmse = 0.12



(b) rmse = 0.14



(c) rmse = 0.15



(d) rmse = 0.16



(e) rmse = 0.16



(f) rmse = 0.18



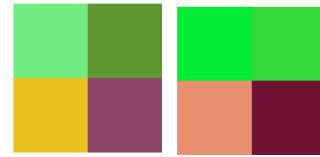
(g) rmse = 0.18



(h) rmse = 0.19



(i) rmse = 0.20



(j) rmse = 0.22

Fig. 4: Reverse-engineered patches compared to original trigger on 10 Trojan models. At each pair, the original patch is on the left while the retrieved one is on the right.

the pure and Trojan models without knowing the potential target class. These scores are presented in Table 3. The lesser the entropy score the more effective the retrieved reverse-engineered mask and trigger, hence it is more possible that the model in test is Trojaned.

Model	<i>Entropy score</i>	
	GTSRB	CIFAR-10
<b>Avg Pure Models</b>	<b>4.95</b>	<b>3.00</b>
set 1	0.003	0.001
set 2	0.004	0.002
set 3	0.004	0.003
set 4	0.005	0.006
set 5	0.003	0.001
<b>Avg Trojan Models</b>	<b>0.004</b>	<b>0.002</b>

Table 3: Entropy score computed based on the mask and patch retrieved by our proposed method on GTSRB and CIFAR-10 dataset.

From Table 3, we observe that the gap between the high scores of the pure models and the low score of Trojan models are significant and stable across multiple settings. This reliability is achieved through the universality of entropy score measure which does not depend on any change in model and data (see Lemma 1). Because of this, it is straightforward with STS to set a robust universal threshold using number of classes and expected Trojan effectiveness to detect the Trojan models using the entropy score.

We compare the performance of STS in detecting Trojan Model with Neural Cleanse (NC)[15] which is the state-of-the-art for this problem. We use the same settings on models and data for both STS and NC. Similar to the entropy score used in STS, NC uses the anomaly index to rank the pureness of the candidate model. These scores of the two methods are shown in Table 4.

Model	GTSRB		CIFAR-10	
	<i>Entropy score</i>	<i>Anomaly Index</i>	<i>Entropy score</i>	<i>Anomaly Index</i>
Pure Models	[4.85, 5.04]	[0.73, 23.30]	[2.55, 3.32]	[0.68, 2.56]
Trojan Models	[0.0, 0.011]	[11.64, 71.08]	[0.0, 0.01 ]	[22.98, 244.94]

Table 4: The minimum and maximum value of entropy scores (ours) and anomaly indexes (NC [15]) of the pure and Trojan models represented as  $[min, max]$ .

In our method, the gap between pure and Trojan area in entropy scores are large and consistent. Meanwhile, the Neural Cleanse’s anomaly index varies in a

bigger range intra-class and close or overlapping inter-class. This again supports that our proposed method can come up with a more robust threshold to detect Trojan models.

Table 5 show the final accuracy of Trojan model detection between our STS and NC. The upper limit of entropy score for GTSRB and CIFAR-10 according to Lemma 1 is 0.1347 and 0.1125 respectively. For STS, we use this scores as the threshold for F1-score computation. For NC, we set the threshold to be 2.0 following recommendation in the method [15].

Measures	GTSRB		CIFAR-10	
	STS (Ours)	NC	STS (Ours)	NC
F1-score	<b>1.0</b>	0.68	<b>1.0</b>	0.96

Table 5: Accuracy (as F1-score) of Trojan Model detection between our method (STS) and NC [15].

### 3.5 Computational Complexity

Beside the effectiveness in accurately detecting the Trojan model and recover the effective triggers, we also measured the complexity and computational cost of the Trojan scanning process. As our method does not make assumption about the target class  $c_t$ , the complexity is constant ( $\mathcal{O}(1)$ ) to this parameter. In the mean time, the state-of-the-art methods such as NC rely on the optimisation process that assumes knowledge about the target class. This results in a loop through all of the possible classes and ends up in a complexity of  $\mathcal{O}(C)$ . Because of this difference in complexity, STS is significantly faster than NC. Concretely, in our experiments, STS takes around 2 hours to detect 10 Trojan models on GTSRB, compared to more than 9 hours that NC took on the identical settings.

## 4 Conclusion and Future work

In this paper, we propose a method to detect Trojan model using trigger reverse engineering approach. We use a method to find out the minimum change that can map all the instances to a target class, for a Trojan model. The experiments conducted on GTSRB and CIFAR-10 show that our proposed method can reverse-engineer visually similar patch with high Trojan effectiveness. We propose a measure, entropy score, to compute the robust upper threshold to detect the Trojan models. We report entropy score and F1-score to support our claims. It is evident from the results that our method is more robust and less computationally expensive compared to the state-of-the-art method.

Future work is possible by generating models which has multiple target classes. Another future possibility is to work on Trojans which are distributed rather than a solid patch. We also found that for a single Trojan model, there exists multiple triggers as solution, so given this we also focus to work on getting a distribution of Trojan triggers for a Trojan model.

## References

1. Chan, A., Ong, Y.S.: Poison as a Cure: Detecting & Neutralizing Variable-Sized Backdoor Attacks in Deep Neural Networks. arXiv preprint arXiv:1911.08040 (2019)
2. Chen, B., Carvalho, W., Baracaldo, N., Ludwig, H., Edwards, B., Lee, T., Molloy, I., Srivastava, B.: Detecting Backdoor Attacks on Deep Neural Networks by Activation Clustering. arXiv preprint arXiv:1811.03728 (2018)
3. Chen, H., Fu, C., Zhao, J., Koushanfar, F.: DeepInspect: A Black-box Trojan Detection and Mitigation Framework for Deep Neural Networks. In: Proceedings of the 28th International Joint Conference on Artificial Intelligence. AAAI Press. pp. 4658–4664 (2019)
4. Gu, T., Dolan-Gavitt, B., Garg, S.: Badnets: Identifying Vulnerabilities in the Machine Learning Model Supply Chain. arXiv preprint arXiv:1708.06733 (2017)
5. Ilyas, A., Engstrom, L., Athalye, A., Lin, J.: Black-box Adversarial Attacks with Limited Queries and Information. arXiv preprint arXiv:1804.08598 (2018)
6. Kingma, D.P., Ba, J.: Adam: A Method for Stochastic Optimization. arXiv preprint arXiv:1412.6980 (2014)
7. Kolouri, S., Saha, A., Pirsiavash, H., Hoffmann, H.: Universal Litmus Patterns: Revealing Backdoor Attacks in CNNs. arXiv preprint arXiv:1906.10842 (2019)
8. Krizhevsky, A.: Learning Multiple Layers of Features from Tiny Images. Tech. rep. (2009)
9. Li, Y., Li, L., Wang, L., Zhang, T., Gong, B.: NATTACK: Learning the Distributions of Adversarial Examples for an Improved Black-Box Attack on Deep Neural Networks. arXiv preprint arXiv:1905.00441 (2019)
10. Liu, Y., Lee, W.C., Tao, G., Ma, S., Aafer, Y., Zhang, X.: ABS: Scanning Neural Networks for Back-doors by Artificial Brain Stimulation. In: Proceedings of the 2019 ACM SIGSAC Conference on Computer and Communications Security. pp. 1265–1282 (2019)
11. Papernot, N., McDaniel, P., Jha, S., Fredrikson, M., Celik, Z.B., Swami, A.: The Limitations of Deep Learning in Adversarial Settings. In: 2016 IEEE European Symposium on Security and Privacy (EuroS&P). pp. 372–387. IEEE (2016)
12. Simonyan, K., Zisserman, A.: Very Deep Convolutional Networks for Large-Scale Image Recognition. arXiv preprint arXiv:1409.1556 (2014)
13. Stallkamp, J., Schlipsing, M., Salmen, J., Igel, C.: Man vs. Computer: Benchmarking Machine Learning Algorithms for Traffic Sign Recognition. Neural Networks pp. 323–332 (2012)
14. Szegedy, C., Zaremba, W., Sutskever, I., Bruna, J., Erhan, D., Goodfellow, I., Fergus, R.: Intriguing properties of neural networks. arXiv preprint arXiv:1312.6199 (2013)
15. Wang, B., Yao, Y., Shan, S., Li, H., Viswanath, B., Zheng, H., Zhao, B.Y.: Neural Cleanse: Identifying and Mitigating Backdoor Attacks in Neural Networks. In: 2019 IEEE Symposium on Security and Privacy (SP). pp. 707–723. IEEE (2019)
16. Xiang, Z., Miller, D.J., Kesidis, G.: Revealing Backdoors, Post-Training, in DNN Classifiers via Novel Inference on Optimized Perturbations Inducing Group Misclassification. arXiv preprint arXiv:1908.10498 (2019)
17. Xu, X., Wang, Q., Li, H., Borisov, N., Gunter, C.A., Li, B.: Detecting AI Trojans Using Meta Neural Analysis. arXiv preprint arXiv:1910.03137 (2019)